Kanglexin, a new anthraquinone compound, attenuates lipid accumulation by activating the AMPK/SREBP-2/PCSK9/LDLR signalling pathway

Xin Li[a,1], Xueling Hu[a,1], Tengfei Pan[b,1], Lei Dong[a], Lili Ding[a], Zhenzhong Wang[d,e], Rui Song[a], Xiuzhu Wang[a], Ning Wang[a,b], Yan Zhang[a], Jinhui Wang[c], Baofeng Yang[a,b,*]

[a] *Department of Pharmacology (State-Province Key Laboratories of Biomedicine - Pharmaceutics of China, Key Laboratory of Cardiovascular Medicine Research, Ministry of Education), College of Pharmacy, Harbin Medical University, Harbin, China*

[b] *Northern Translational Medicine Research and Cooperation Center, Heilongjiang Academy of Medical Sciences, Harbin Medical University, Harbin, Heilongjiang*

150081, China

[c] *Department of Medicinal Chemistry and Natural Medicine Chemistry, College of Pharmacy, Harbin Medical University, Harbin, Heilongjiang 150081, China* [d] *Jiangsu Kanion Pharmaceutical CO. LTD, Jiangsu, Lianyungang 222001, China* [e] *State Key Laboratory of New-tech for Chinese Medicine Pharmaceutical Process, Jiangsu, Lianyungang 222001, China*

ARTICLEINFO

Keywords:
Anthraquinone compound
Kanglexin
Hyperlipidaemia
Fatty liver
AMPK/SREBP-2/PCSK9/LDLR signalling pathway

ABSTRACT

Hyperlipidaemia is one of the major risk factors for atherosclerosis, coronary heart disease, stroke and diabetes. In the present study, we synthesized a new anthraquinone compound, 1,8-dihydroxy-3-succinic acid monoethyl ester-6-methylanthraquinone, and named it Kanglexin (KLX). The aim of this study was to evaluate whether KLX has a lipid-lowering effect and to explore the potential molecular mechanism. In this study, Sprague-Dawley rats were fed a high fat diet (HFD) for 5 weeks to establish a hyperlipidaemia model; then, the rats were orally administered KLX (20, 40, and 80 mg $kg^{-1}.d^{-1}$) or atorvastatin calcium (AT, 10 mg $kg^{-1}.d^{-1}$) once a day for 2 weeks. KLX had prominent effects on reducing blood lipids, hepatic lipid accumulation, body weight and the ratio of liver weight/body weight. Furthermore, KLXdramatically reduced the total cholesterol (TC) and triglyceride (TG) levels and lipid accumulation in a HepG2 cell model of dyslipidaemia induced by 1 mmol/L oleic acid (OA). KLX may decrease lipid levels by phosphorylating adenosine monophosphate-activated protein kinase (AMPK) and the downstream sterol regulatory element binding protein 2 (SREBP-2)/proprotein convertase subtilisin/kexin type 9 (PCSK9)/low-density lipoprotein receptor (LDLR) signalling pathway in the HFD rats and OA-treated HepG2 cells. The effects of KLX on the AMPK/SREBP-2/PCSK9/LDLR signalling pathway were abolished when AMPK was inhibited by compound C (a specific AMPK inhibitor) in HepG2 cells. In summary, KLX has an efficient lipid-lowering effect mediated by activation of the AMPK/SREBP-2/PCSK9/LDLR signalling pathway. Our findings may provide new insight into and evidence for the discovery of a new lipid-lowering drug for the prevention and treatment of hyperlipidaemia, fatty liver, and cardiovascular disease in the clinic.

Abbreviations: ACC, acetyl-CoA carboxylase; ACLY, ATP-citrate lyase; AICAR, 5-aminoimidazole-4-carboxamide ribonucleoside; FASN, fatty acid synthase; AMPK, adenosine monophosphate activated protein kinase; HDL-c, high-density lipoprotein cholesterol; HFD, high-fat diet; HMGCR, 3-hydroxy-3-methylglutaryl-CoA reductase; HSL, hormone-sensitive lipase; KLX, Kanglexin, the name of 1, 8-dihydroxy-3-succinic acid monoethyl ester-6-methylanthraquinone; LDL-c, low-density lipoprotein cholesterol; LDLR, low-density lipoprotein receptor; OA, oleic acid; PBS, phosphate buffer saline solutions; PCSK9, proprotein convertase subtilisin/kexin type 9; SREBP, sterol regulatory element binding protein; TC, total cholesterol; TG, triglyceride.

* Corresponding author: Department of Pharmacology (State-Province Key Laboratories of Biomedicine - Pharmaceutics of China, Key Laboratory of Cardiovascular Medicine Research, Ministry of Education), College of Pharmacy, Harbin Medical University, Harbin, China.

E-mail addresses: lixin@hrbmu.edu.cn (X. Li), 596423749@qq.com (X. Hu), tf1002@qq.com (T. Pan), 785749485@qq.com (L. Dong), 1902164632@qq.com (L. Ding), wzh-nj@163.com (Z. Wang), 438863779@qq.com (R. Song), 1450126244@qq.com (X. Wang), wangning@ems.hrbmu.edu.cn (N. Wang), zhangyan@ ems.hrbmu.edu.cn (Y. Zhang), 15999290001@163.com (J. Wang), yangbf@ems.hrbmu.edu.cn (B. Yang). [1] With equal contribution to this work.

https://doi.org/10.1016/j.biopha.2020.110802
Received 12 May 2020; Received in revised form 16 September 2020; Accepted 25 September 2020
Available online 14 November 2020
0753-3322/© 2020 The Author(s). Published by Elsevier Masson SAS. This is an open access article under the CC BY-NC-ND license (http://creativecommons.org/licenses/by-nc-nd/4.0/).

1. Introduction

Hyperlipidaemia is a metabolic disorder characterized by abnormal levels of lipids or lipoproteins with elevated levels of total cholesterol (TC), triglyceride (TG) and low density lipoprotein cholesterol (LDL-c) and decreased levels of high density lipoprotein cholesterol (HDL-c) [1, 2]. Continuously high blood lipid levels can cause a number of cardiovascular and cerebrovascular diseases, such as atherosclerosis, coronary heart disease, stroke and diabetes [3–5]. Currently, a number of hypolipidaemic agents are used to treat hyperlipidaemia, such as 3-hydroxy-3-methylglutaryl-CoA reductase (HMGCR) inhibitors, fibrates, nicotinic acid and cholesterol absorption inhibitors [6–8]. However, control of the blood lipid levels remains unsatisfactory worldwide and the number of people with dyslipidaemia is expected to reach 78 million in the major countries by the year 2022 [9]. Therefore, development and discovery of new drugs against hyperlipidaemia is of great significance.

Anthraquinones are the active ingredients of a number of Chinese herbal medicines and are mainly present in certain species of the families Polygonaceae, Rubiaceae, and Leguminosae, such as *Rheum palmatum L., Rubia cordifolia L., Polygoni multiflori*, *Polygonum cuspidatum*, and *Semen Cassiae* [10]. Numerous studies have demonstrated that plants rich in anthraquinones or anthraquinone extracts have anticancer [11,12] anti-inflammatory [13,14], lapactic [15] and lipid lowering effects [16–18]. Anthraquinones extracted

from Chinese herbal medicines are present mainly in the crude extracts, and the contents of the anthraquinone compounds are low [19]. The purification of anthraquinones from Chinese herbal medicines frequently employs organic solvents, such as ether, benzene and chloroform, which are flammable, explosive, toxic, and harmful [20,21]. The content of anthraquinones can exceed 50 %; however, the residual solvent in the extract will cause major toxicity in humans. The extraction methods are dangerous, cause pollution and are not suitable for mass production. In this study, we synthesized a new anthraquinone compound 1,8-dihydroxy-3-succinic acid monoethyl ester-6-methylanthraquinone through an innovative synthetic route. We named the compound Kanglexin (KLX).

Adenosine monophosphate-activated protein kinase (AMPK) is the key molecule in the regulation of biological energy metabolism and is the focus of the studies on metabolism-related diseases [22]. AMPK can regulate lipid metabolism by influencing the expression of the downstream target genes, including sterol regulatory element binding protein 2 (SREBP-2) [23]. The SREBP-2/PCSK9/LDLR signalling pathway is a novel and effective pathway that regulates lipid metabolism [24].

The aim of this study was to synthesize a new anthraquinone compound, then to evaluate whether it has a lipid-lowering effect and to explore the potential molecular mechanism. We hypothesized that KLX may reduce lipid accumulation by activating the hepatic AMPK/SREBP-2/PCSK9/LDLR signalling pathway. This result may provide a new compound for discovery of drug treatment of hyperlipidaemia or fatty liver.

2. Materials and methods

2.1. Synthesis of 1,8-dihydroxy-3-succinic acid monoethyl ester-6-methyl anthraquinone

1,8-Dihydroxy-3-succinic acid monoethyl ester-6-methylanthraquinone (Kanglexin, KLX) used in this study was synthesized by Department of Pharmacology (State-Province Key Laboratories of Biomedicine - Pharmaceutics of China, Key Laboratory of Cardiovascular Medicine Research, Ministry of Education), College of Pharmacy, Harbin Medical University.

The scheme of the synthetic route of 1,8-dihydroxy-3-succinic acid monoethyl ester-6-methylanthraquinone is shown in Fig. 1**A**.

2.1.1. Synthesis of monoethyl succinate

Succinic anhydride was placed in a round-bottom flask with ethyl alcohol as a solvent. The optimal ratio of succinic anhydride to ethanol volume was 1:4. The mixture was reflux heated for 4 h and excess of ethanol was removed by vacuum distillation to obtain light yellow oily succinate monoethyl ester. The product was not separated and used in the next step.

2.1.2. Synthesis of ethyl succinyl chloride

Monoethyl succinate was placed in a round-bottom flask with thionyl chloride as a solvent. The mass ratio of monoethyl succinate to thionyl chloride was 1:4. The mixture was reflux heated for 2 h and excess thionyl chloride was removed by vacuum distillation to obtain light yellow oily ethyl succinyl chloride. The product was not separated and used in the next step.

2.1.3. Synthesis of raw product of 1,8-dihydroxy-3-succinic acid monoethyl ester-6-methylanthraquinone

Emodin and alkali were placed in a round bottom flask with methylene chloride as a solvent. The alkali can be pyridine, triethylamine or ammonia liquor; ammonia liquor is optimal. Ethyl succinyl chloride was slowly added into the round bottom flask. The mass ratio of emodin to succinic acid monoethyl chloride was 1:0.5 ~ 1:1; the optimal ratio was 1:0.7. The reaction was performed at room temperature. Extraction was performed with aqueous solution of sodium bicarbonate. Organic phase was combined and extracted with saturated salt water. Organic phase was combined, dried with anhydrous sodium sulfate, filtered and condensed under a reduced pressure. The raw product of 1,8-dihydroxy- 3-succinic acid monoethyl ester-6-methylanthraquinone was obtained as a violet yellow solid.

2.1.4. Purification of 1,8-dihydroxy-3-succinic acid monoethyl ester-6- methylanthraquinone

Silica gel column chromatography was used for elution of the crude product with a mixture of dichloromethane and

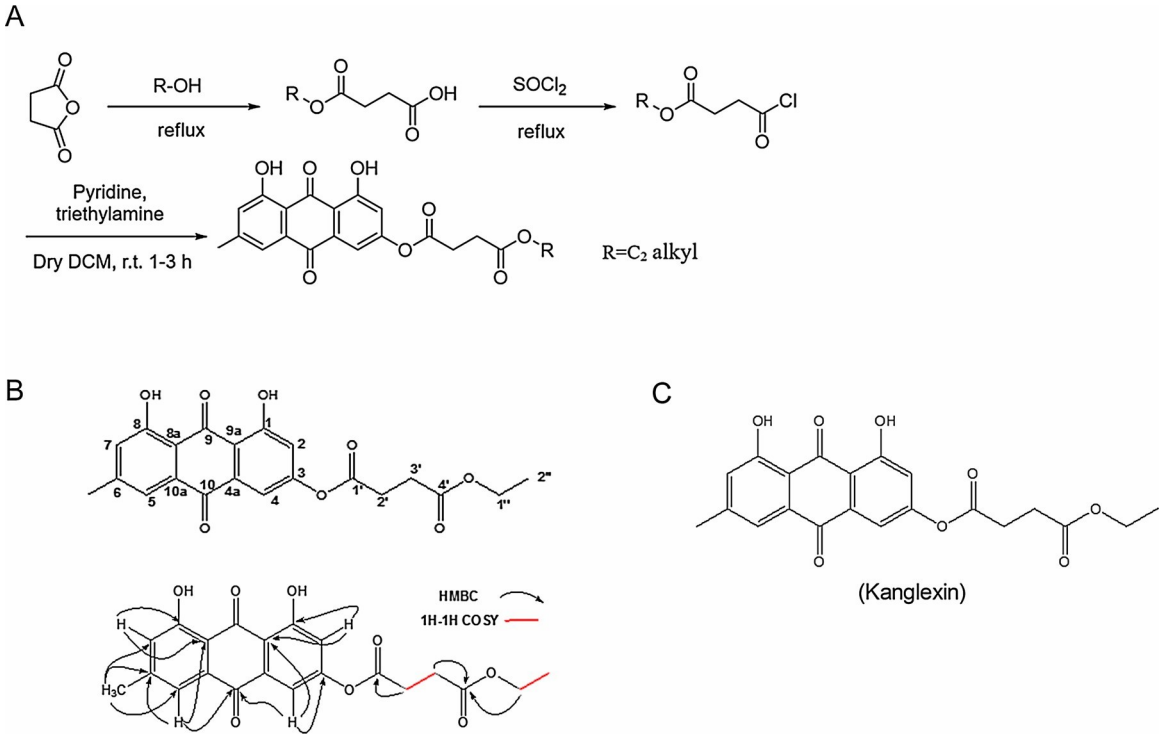

Fig. 1. The Scheme of the Synthetic Route and Structural Identification of 1,8-Dihydroxy-3-succinic acid monoethyl ester-6-methylanthraquinone (Kanglexin). (A) Scheme of synthetic route of KLX. (B) Schematic diagram of two-dimensional NMR correlation signals of KLX. (C) The chemical structure of KLX. KLX: Kanglexin, name of the compound 1,8-Dihydroxy-3-succinic acid monoethyl ester-6-methylanthraquinone.

methanol. The volume ratio of dichloromethane to methanol was 100:1 ~ 100:100; the ratio of 100:1 was optimal. A light yellow product was purified Kanglexin.

2.2. Identification of the structure of 1,8-dihydroxy-3-succinic acid monoethyl ester-6-methylanthraquinone

The structure of 1,8-dihydroxy-3-succinic acid monoethyl ester-6- methylanthraquinone was identified by ultraviolet (UV) absorption, infrared (IR) absorption, ^{1}H-nuclear magnetic resonance (^{1}H-NMR), ^{13}C- nuclear magnetic resonance (^{13}C-NMR), distortionless enhancement by polarization transfer (DEPT), AV-600-COSY, AV-600-HSQC and AV-600- HMBC spectroscopy after the synthesis.

2.3. Hyperlipidaemia models and drug treatment

Thirty-six male Sprague-Dawley (SD) rats (8-week-old, 200 ± 20 g body weight) of SPF grade were obtained from Liaoning Longevity Biotechnology Co., Ltd. (Liaoning, China). Rats were housed at 23 ± 2 °C in a room with 55 ± 5% humidity maintained on a 12 h artificial dark- light cycle (lights on at 07:00 A.M.) and were provided free access to food and water. Original studies in the animals have been carried out in accordance with the U.K. Animals (Scientific Procedures) Act, 1986 and associated guidelines, the National Institutes of Health guide for the care and use of laboratory animals (NIH Publications No.8023, revised 1978), and the Institutional Animal Care and Use Committee of Harbin Medical University.

After one week of maintenance feeding, the SD rats were randomly divided into a control group (n = 6) and a hyperlipidaemia model group (n = 30). Rats in the control group were fed with maintenance food (Keao Xieli, Beijing, China) throughout the experiment. Rats in the hyperlipidaemia model group were fed with a high fat diet (maintenance food supplemented with 20 % sucrose, 15 % lard oil, 1.2 % cholesterol, and 0.2 % sodium tauroglycocholate, Huafukang, Beijing, China) for 5 weeks. Then, blood samples were collected from the tail vein of each rat and the serum levels of TC, TG, HDL-c and LDL-c were measured using an automatic biochemical analyser (Hitachi, Tokyo, Japan).

According to the levels of TC, TG and LDL-c, the hyperlipidaemia model rats were then randomly divided into five groups including the hyperlipidaemia model group (HFD, n = 6), atorvastatin calcium group (10 mg kg^{-1}·d^{-1}, AT, n = 6), low dose of KLX group (20 mg kg^{-1}·d^{-1}, KLX-L, n = 6), medium dose of KLX group (40 mg kg^{-1}·d^{-1}, KLX-M, n = 6) and high dose of KLX group (80 mg kg^{-1}·d^{-1}, KLX-H, n = 6). All groups of rats excepted the control group were fed with HFD throughout the experiment. Atorvastatin calcium (Pfizer, New York, USA) and KLX were dissolved in 0.5 % carboxymethyl cellulose-Na (CMC-Na, Fuchen Chemical Reagent, Tianjin, China). Drugs were orally administered to the corresponding rats once a day for 2 weeks. Rats in the control and hyperlipidaemia model groups were administered the same volume of CMC-Na. Body weight of the rats was measured weekly. Rats were sacrificed on day 14 after the treatment with the drugs; the serum was collected from the abdominal aorta and the liver tissue was collected for other experiments. *2.4. Lipid content determination*

The serum levels of TC, TG, HDL-c and LDL-c were detected with the corresponding TC, TG, HDL-c and LDL-c kits (Sichuan Maccura, Chengdu, China) using a Hitachi 7100 automatic biochemical analyser.

Liver tissue samples were homogenized in phosphate-buffered saline (PBS). HepG2 cells used in the experiments were collected with trypsin (Solarbio, Beijing, China) and lysed with 2% Triton X-100 (Amresco, Washington, USA) for 30–40 min. Then, the lipid extracts from the tissue or cells were analysed with the TC and TG diagnostic kits (Jiancheng Bioengineering Institute, Nanjing, China). Total protein concentrations in the liver tissue or cells were determined using a BCA protein assay kit (Beyotime, Shanghai, China) with an internal standard. Then, the TC and TG contents of the liver homogenates and cell lysates were detected by measuring the absorbance at 510 nm using a microplate reader (BioTek, Vermont, USA) and reported as mmol/g of protein according to the manufacturer's instructions.

2.5. Oil Red O staining

Rat liver tissues were cut into slices with a thickness of 7 μm using a cryostat microtome (Leica, Wetzlar, Germany). If HepG2 cells were used, the cells were plated on the coverslips in six-well plates. After reaching 80 % confluence, the cells were washed with PBS for 10 min at room temperature. Then, the cells were fixed with a 4% paraformaldehyde solution (Biosharp, Hefei, China). Samples were washed with distilled water and stained with an Oil Red O kit (Jiancheng Bioengineering Institute, Nanjing, China) according to the manufacturer's instructions. Briefly, samples were incubated with the reagent 1 for 15 min, counterstained with reagent 2 for 3− 5 min, and finally covered with glycerine gelatine (reagent 3). Images were captured with a microscope (Nikon, Tokyo, Japan).

2.6. Haematoxylin-eosin staining

Samples of the fresh liver tissue were fixed with 10 % neutral formalin (Tianli Chemical Reagents, Tianjin, China), dehydrated, embedded in paraffin and sectioned into 5 μm slices. Then, the sections were stained with a haematoxylin and eosin kit (Beyotime, Shanghai, China). Sections were washed with distilled water, dehydrated and covered with neutral gum. Images were captured with a microscope (Nikon, Tokyo, Japan) for the pathological analysis.

2.7. Cell culture and treatment

Human hepatocellular carcinoma cell line HepG2 was obtained from the American Type Culture Collection (ATCC, Manassas, USA). Cells were cultured in Dulbecco's Modified Eagle's Medium (DMEM, HyClone, Logan, USA) supplemented with 10 % foetal bovine serum (FBS, Biological Industries, Kibbutz Beit Haemek, Israel) and 1% penicillin and streptomycin solution (HaiGene, Harbin, China). After reaching 80 %–90 % confluence, cells were incubated with 1 mmol/L OA (Sigma, St. Louis, MO, USA) for 24 h to establish a hyperlipidaemia cell model and treated with atorvastatin calcium (1 μmol/L, AT, Sigma, St. Louis, MO, USA) or KLX (5 μmol/L, 10 μmol/L and 20 μmol/L) for 24 h. Cells were always exposed to OA during drug treatment. To explore whether AMPK is necessary for KLX exerting its function, specific AMPK inhibitor, compound C (Merck, Darmstadt, Germany), was used to block AMPK activation. Cells were incubated with compound C (10 μmol/L), KLX (10 μmol/L) or compound C (10 μmol/L) plus KLX (10 μmol/L) for 24 h.

2.8. Western blot

Total protein samples were extracted from the rat liver or HepG2 cells with RIPA buffer (Beyotime, Shanghai, China). Total protein concentrations were measured using a BCA protein assay kit (Beyotime, Shanghai, China). Protein samples (80 μg) were fractionated by sodium dodecylsulfate polyacrylamide gel electrophoresis through the 10 % gels to determine the levels of adenosine monophosphate-activated protein kinase (AMPK), phosphorylated adenosine monophosphate activated protein kinase (p-AMPK, phospho Thr172), proprotein convertase subtilisin/kexin type 9 (PCSK9), the precursor forms of sterol regulatory element binding protein 2 (P-SREBP-2), the nuclear forms of sterol regulatory element binding protein 2 (N-SREBP-2), and low density lipoprotein receptor (LDLR). Proteins were then transferred onto nitrocellulose membranes (Pall Corporation, New York, USA), which were blocked with 5% non-fat dry milk (BD Difco, New Jersey, USA) for 2 h at room temperature. The following primary antibodies were incubated with the membrane overnight at 4 °C: anti-AMPK (1:1000, ab80039, Abcam, MA, USA, 62 kDa), anti-Thr172 p-AMPK (1:1000, ab195946, Abcam, MA, USA, 62 kDa), anti-SREBP-2 (1:500, ab30682, Abcam, MA, USA, 126 kDa, 68 kDa), anti-PCSK9 (1:1000, ab52754, Abcam, MA, USA, 58 kDa), anti-LDLR (1:1000, ab30532, Abcam, MA USA, 130 kDa) and anti-β-actin (1:1000, Bioss, bs0061R, Beijing, China, 43 kDa) as an internal control for total protein. Membranes were washed with PBST and then incubated with an appropriate secondary antibody (LI-COR Bioscience, Lincoln, NE, USA) for 50 min at room temperature. Finally, the western blot bands were scanned with an Odyssey infrared imaging system (LI-COR Biosciences, Lincoln, NE, USA) and quantified using the Odyssey v1.2 software by measuring the band intensity (area × OD) in each group normalizing the values to the β-actin signal.

2.9. Quantitative real-time RT-PCR

Total RNA samples were extracted from HepG cells or liver using Trizol reagent (Invitrogen, Carlsbad, USA). The mRNA expression levels of SREBP-2 were tested by using a FastStart universal SYBR Green master (Rox) (Roche, Mannheim, Germany) using an ABI 7500 fast real time PCR system (Applied Biosystems, Foster City, USA). β-Actin was used as an internal control of SREBP-2. Relative expression was determined using the $2^{-\Delta\Delta CT}$ method. The primers were synthesized by Invitrogen and the sequences were as follows:

SREBP-2-F: 5′-GGTACGCTGGTTACTCAAAAAGGT-3′; SREBP-2-R: 5′– CCCTCGCACTGCTCTTAGCT-3′; β-actin-F: CCTGTGGCATCCATGAAACTAC; β-actin-R: CCAGGGCAGTAATCTCCTTCTG.

2.10. Statistical analysis

Data are presented as the mean ± standard error of the mean (SEM). The statistical significance of the differences was analysed using the GraphPad 7 and Microsoft Office software. One-way analysis of variance (ANOVA) was used to compare more than two groups, and differences with a p value < 0.05 were considered statistically significant.

3. Results

3.1. Structural Identification of 1,8-dihydroxy-3-succinic acid monoethyl ester-6-methylanthraquinone

The structure of the compound was identified, and the results indicate that the compound was 1,8-dihydroxy-3-succinic acid monoethyl ester-6-methylanthraquinone, a yellow powder that is soluble in methanol; $[\alpha]^{26}_{D}$ 0.0° (*c* 0.5, $CHCl_3$)· IR (KBr, cm^{-1}) 3500 (− OH), 3088 (Ar-H), 2981 (RH), 1763 (C¯–O), 1730 (C¯–O), 1624 (benzene ring), 1481 (benzene ring) (Fig. S1). UV [nm (log e), MeOH]: 278 (3.37), 268 (3.40) (Fig. S2). CD (nm, △ε, MeOH): 212 (− 0.56). ^{1}H-NMR (Fig. S3), δ 7.08 (1H, d, J=2.2 Hz), 7.33 (1H, d, J=2.2 Hz) is the proton signal of the interstitial coupling on the benzene ring, δ 7.39 (1H, brs), 7.07 (1H, brs) is the aromatic proton signal, δ 2.91 (2H, d, J = 6.2), 2.71 (2H, d, J=6.2 Hz), 4.13 (2H, q, J=7.1 Hz) are three methylene proton signals, δ 2.36 (3H, s), 1.22 (3H, t, J=7.1 Hz) is the methyl proton signal. ^{13}C-NMR spectrum (Fig. S4) showed 21 carbon signals; δ 190.8, 181.0 is the ketone carbonyl carbon signal, δ 172.0, 170.6 is the ester carbonyl carbon signal, 163.2, 162.0, 157.0 is the oxygen-carbon signal on the benzene ring. ^{1}H-^{1}H COSY spectrum, δ 2.91, 2.71 had the relevant signals, δ 4.13, 1.22 had a relevant signal (Fig. S5). The distortionless enhancement by polarization transfer (DEPT) spectrum of the compound (Fig. S6) indicates that the structure contains four instances of sp2 hybridization of methyl carbon signals, twelve quaternary carbon signals with sp2 hybridization, three sp3-hybridized methylene carbon signals, and two methyl carbon signals. Hydrocarbon signals were classified by heteronuclear multiple quantum coherence (HMQC) (Fig. S7). The result of heteronuclear multiple-bond correlation (HMBC) (Fig. S8) showed that δ7.08 proton has a remote correlation with the chemical displacement of 163.2 and 114.3, δ7.33 proton has a remote correlation with carbon signals 157.0, 181.0, and 114.3, δ7.39 proton has a remote correlation to the carbon signal of δ149.5, 181.0, 113.8, δ7.07 proton has a remote correlation to the carbon signal of δ162.2, 113.8. δ2.91 proton has a remote correlation to the carbon signal of δ170.6, δ2.71 proton has a remote correlation to the carbon signal of δ172.2, δ4.13 proton has a remote correlation to the carbon signal of δ172.2, δ1.22 proton has a remote correlation to the carbon signal of δ60.7, 2.36 methyl protons have a remote correlation to the carbon signal of 121.1, 149.5, 116.7. The structure of the compound was determined by combining the information; signal assignment is shown in Table 1. Schematic diagram of two-dimensional NMR correlation signals is shown in Fig. 1**B**. These results indicates the compound is 1,8-dihydroxy-3-succinic acid monoethyl ester-6-methylanthraquinone (Kanglexin, KLX). The chemical structure of KLX is shown in Fig. 1**C**; with the molecular formula: $C_{21}H_{18}O_8$, molecular weight: 398.

3.2. Lipid-lowering effect of Kanglexin (KLX) in hyperlipidaemic rats

After chronic consumption of a high fat diet (HFD) for 5 weeks, the body weight (Fig. 2**A**) and serum levels of total cholesterol (TC, Fig. 2**B**), triglycerides (TG, Fig. 2**C**) and low density lipoprotein cholesterol (LDL- c, Fig. 2**D**) of HFD-fed rats were significantly increased compared to the values detected in the normal rats. These data suggest that a rat model of hyperlipidaemia was successfully established. Then, the rats

were continuously treated with the corresponding drugs using the same feed supply. All rats except the control group were fed with HFD. After 2 weeks of drug treatment, administration of KLX at various doses significantly reduced the body weight (Fig. 2**E**) and the ratio of liver weight/body weight in a dose-dependent manner (Fig. 2**F**) compared with the values detected in the HFD-fed rats. Low (KLX-L, 20 mg $kg^{-1}.d^{-1}$), medium (KLX-M, 40 mg $kg^{-1}.d^{-1}$) or high doses of KLX (KLX- H, 80 mg $kg^{-1}.d^{-1}$) treatment dramatically decreased the serum levels of TC by 28.3 %, 32.5 % and 43.3 %, TG by 18.8 %, 32.4 % and 41.4 %, and LDL-c by 38.9 %, 38.2 % and 36.6 %, respectively. The effect of 80

Table 1
NMR data of 1, 8-dihydroxy-3-succinic acid monoethyl ester-6-methylanthraquinone (600MHz, DMSO-d6).

Position	^{1}H-NMR	^{13}C-NMR	DEPT	1H-1H COSY	HMBC
1	-	163.2	C	-	-
2	7.08 (1H, d, *J* =2.2Hz)	124.6	-CH-	H-4	C-1,9a
3	-	157.0	C	-	-
4	7.33 (1H, d, *J* =2.2Hz)	113.4	-CH-	H-2	C-3,10,9a
5	7.39 (1H, brs)	121.1	-CH-	H-7	C-6,10,8a
6	-	149.5	C	-	-
7	7.07 (1H, brs)	116.7	-CH-	H-5	C-8, 8a
8	-	162.0	C	-	-
9	-	190.8	C	-	-
10	-	181.0	C	-	-
4a	-	135.0	C	-	-
8a	-	113.8	C	-	-
9a	-	114.3	C	-	-
10a	-	135.0	C	-	-
1′	-	170.6	C	-	-
2′	2.91 (2H, d, *J* =6.2)	29.5	$-CH_2-$	H-2″	C-1″
3′	2.71 (2H, d, *J* =6.2Hz)	29.0	$-CH_2-$	H-3″	C-4′
4′	-	172.2	C	-	-
1″	4.13 (2H, q, *J* =7.1Hz)	60.7	$-CH_2-$	H-1‴	C-4′
2″	1.22 (3H, t, *J* =7.1Hz)	14.5	$-CH_3$	H-2‴	C-1”
6-CH_3	2.36 (3H, s)	22.0	$-CH_3$	-	C-5,6,7

mg $kg^{-1}.d^{-1}$ KLX was equivalent to the effect of atorvastatin calcium, a positive control drug (Fig. 2**E**–**I**). These data suggest that KLX has an efficient lipid-lowering effect on hyperlipidaemic rats in a dose- dependent manner.

3.3. KLX alleviates hepatic lipid accumulation in hyperlipidaemic rats and hepatocytes stimulated by oleic acid

The liver is an important organ for lipid synthesis and metabolism [25]; therefore, we further assessed the effect of KLX on a reduction in the hepatic lipid levels in hyperlipidaemic rats. H&E staining results indicate the presence of well-arranged hepatic cords and hepatocytes with a regular morphology in the liver of normal rats. Additionally, infiltration of inflammatory cells was not observed in the hepatic lobes. In contrast, the livers of the hyperlipidaemic rats were severely injured. The hepatic cords exhibited a disordered arrangement; the hepatocytes were swollen, and a large number of fat vacuoles were observed (Fig. 3**A**). The Oil Red O staining revealed an increase in the number of the lipid droplets in the livers of hyperlipidaemic rats compared with that detected in the livers of normal rats (Fig. 3**B**). Furthermore, TC and TG levels were increased in the livers of hyperlipidaemic rats (Fig. 3**C** and **D**). After the hyperlipidaemic rats were administered KLX, the fat vacuoles and lipid accumulation in the liver were reduced in a dose-dependent manner (Fig. 3**A** and **B**); all doses of KLX decreased the levels of hepatic TC (by 63.2 %, 72.8 % and 81.7 %, respectively) and TG (by 47.7 %, 59.0 % and 64.9 %, respectively) compared with those in the hyperlipidaemic rats (Fig. 3**C** and **D**). The same results were obtained in rats treated with the positive control drug (AT). Thus, KLX can efficiently alleviate hepatic lipid accumulation in hyperlipidaemic rats.

In vitro, HepG2 cells were treated with oleic acid (OA) to establish a hyperlipidaemic hepatocyte model and investigate the lipid-lowering

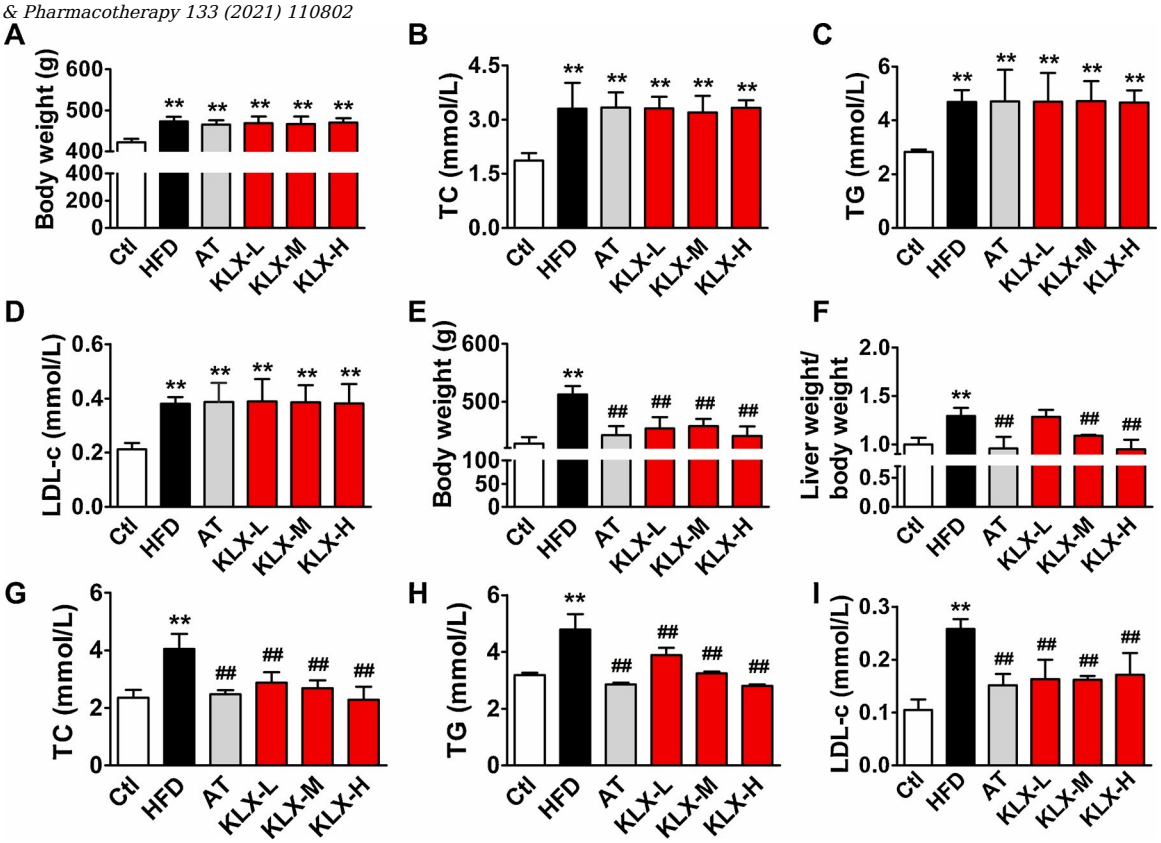

Fig. 2. Lipid-lowering Effect of Kanglexin in Hyperlipidaemic Rats. Body weight **(A)** and the levels of total cholesterol (TC) **(B)**, triglycerides (TGs) **(C)** and low- density lipoprotein cholesterol (LDL-c) **(D)** in the serum of rats after administration of high fat diet for 5 weeks. Body weight **(E)**, liver weight/body weight ratio **(F)**, and the levels of TC **(G)**, TGs **(H)** and LDL-c **(I)** in the serum of hyperlipidemic rats after administration of Kanglexin (KLX) or atorvastatin calcium (AT). All values are shown as the mean ± SEM; n = 8-11, $^{**}P < 0.01$ *vs.* Ctl, $^{\#\#}P < 0.01$ *vs.* HFD. Ctl: control group; HFD: high fat diet group.

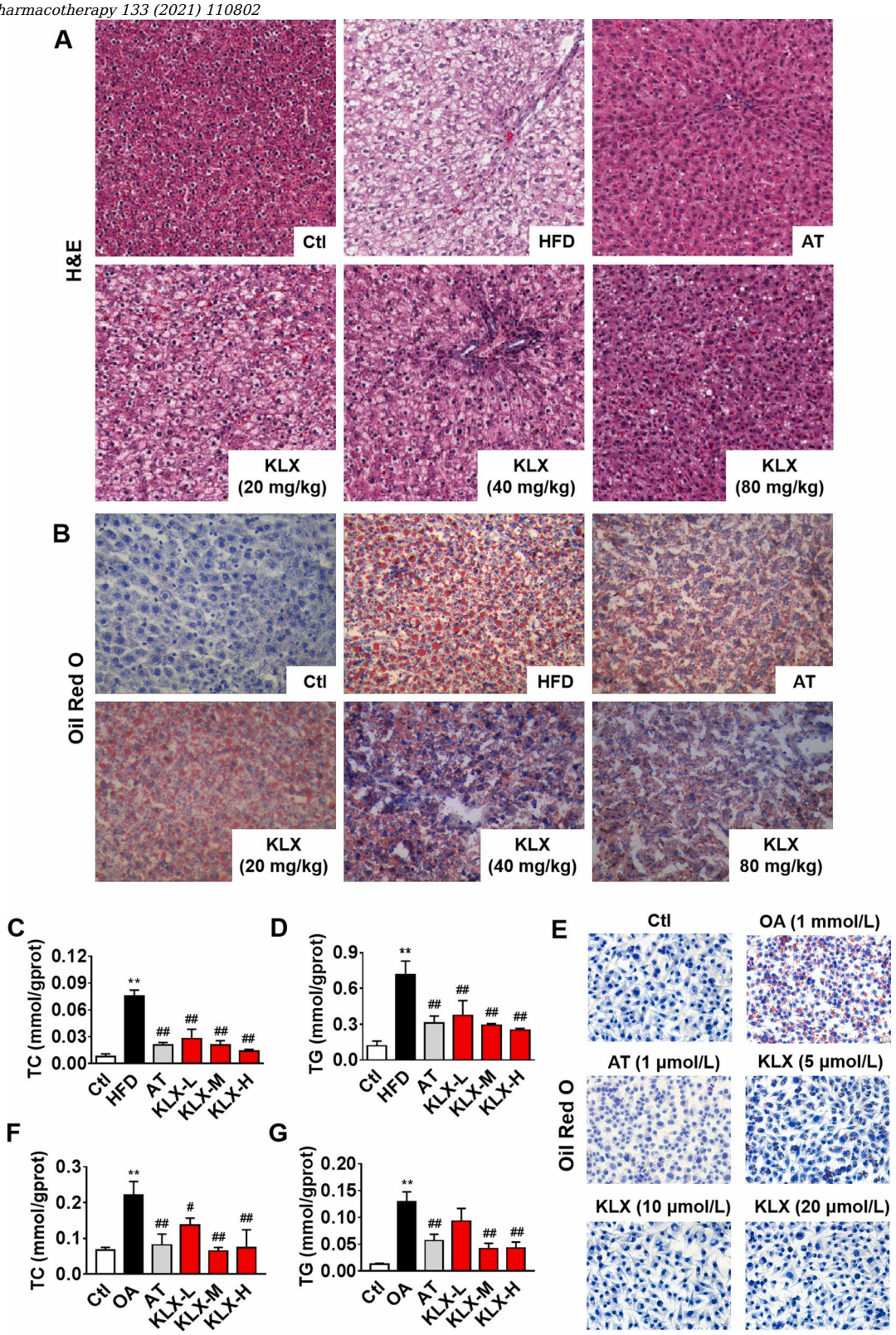

Fig. 3. Kanglexin Alleviates Hepatic Lipid Accumulation in Hyperlipidaemic Rats and Hepatocytes Stimulated with Oleic Acid. Representative H&E staining **(A)** and Oil Red O staining **(B)** of the liver and the hepatic TC **(C)** and TGs **(D)** levels in rats of different groups containing Ctl group, HFD group, atorvastatin calcium (AT) group and three doses of KLX groups. All values are presented as the mean ± SEM; n = 6 - 8, $^{**}P < 0.01$ *vs*. Ctl, $^{\#\#}P < 0.01$ *vs*. HFD. Oil Red O staining **(E)** and TC **(F)** and TGs **(G)** levels in normal hepatocytes (Ctl), dyslipidemic hepatocytes induced by oleic acid (OA), and KLX- or AT-treated hepatocytes. $n = 3$, $^{**}P < 0.01$ *vs*.
Ctl, $^{\#}P < 0.05$, $^{\#\#}P < 0.01$ *vs*. OA. Ctl: control group; OA: oleic acid treatment group; KLX: Kanglexin treatment group; AT: atorvastatin calcium treatment group (For interpretation of the references to colour in this figure legend, the reader is referred to the web version of this article).

effect of KLX. Oil Red O staining indicated that 1 mmol/L OA signifi- receptor (LDLR) protein to regulate cholesterol homeostasis and LDL-c cantly increased the number of lipid droplets (Fig. 3**E**) and the levels of metabolism [27]. Therefore, we determined whether the TC and TG in HepG2 cells (Fig. 3**F**–**G**). Then, HepG2 cells were co- SREBP-2/PCSK9/LDLR signalling pathway, a downstream pathway of incubated with OA and various concentrations of KLX (5, 10 and 20 AMPK, is responsible for the protective effects of KLX in hyperμmol/L), and the number of the cellular lipid droplets was significantly lipidaemia. We found that the expression levels of SREBP-2 mRNA, decreased compared with that in the OA-treated cells (Fig. 3**E**). All doses precursor SREBP-2 (P-SREBP-2) protein, nuclear active form of SREBP-2 of KLX significantly decreased the levels of hepatocyte TC (by 38.0 %, (N-SREBP-2) protein, and PCSK9 proteins were significantly increased, 70.8 % and 66.7 %, respectively) and TG (by 27.7 %, 67.3 % and 66.7 %, and the expression levels of LDLR protein were dramatically decreased respectively) (Fig. 3**F**–**G**) in cells co-treated with OA and KLX compared in the livers of hyperlipidaemic rat compared to the levels in the normal with that in the OA-treated cells. Similar results were obtained in the rats. However, the changes in the relative expression levels of SREBP-2 cells treated with the positive control drug. Thus, KLX can alleviate mRNA and P-SREBP-2, N-SREBP-2, PCSK9 and LDLR proteins were

hepatic lipid accumulation in hyperlipidaemic rats and hepatocytes reversed by KLX (80 mg kg^{-1}·d^{-1}) in the livers of the hyperlipidaemic stimulated by oleic acid. rats (Fig. 5**A**–**F**). Then, we detected the effects of KLX in OA-treated

HepG2 cells. In contrast to the normal cells, the expression

levels of *3.4. KLX promotes AMPK activation* SREBP-2 mRNA and P-SREBP-2, N-SREBP-2 and PCSK9 proteins were significantly

increased, and the LDLR protein expression was decreased

including lipid metabolism [by detecting the levels of the phosphorylated AMPK (p-AMPK, Thr-172) and total AMPK protein to investigate whether the activation of AMPK and its downstream signalling pathway is involved in the protective AMPK activation plays an

important role in energy metabolism, 19]. AMPK activity in the liver was assessed μlipidaemic rats and OA-treated hepatocytes, which is crucial for the role of AMPK in the lipid metabolism. in the OA-treated cells. These effects were also reversed by KLX (10

SREBP-2/PCSK9/LDLR signalling pathway in the livers of hypermol/L) (Fig. 5**G**–**L**). These data indicated that KLX can regulate the -

effects of KLX in hyperlipidaemia. As shown in Fig. 4**A** and **C**, hepatic

p-AMPK levels were decreased in hyperlipidaemic rats compared with the levels in the normal rats; however, p-AMPK expression levels were increased from 0.53 ± 0.12 to 0.88 ± 0.16 in the KLX-treated hyper-*3.6activating AMPK . KLX regulates the SREBP-2/PCSK9/LDLR signalling pathway by*

μlipidaemic rats compared with that in the hyperlipidaemic rats. However, the level of the total AMPK protein in the rat liver was not significantly changed in the control, HFD and KLX (80 mg kgtreatment groups (0.56on AMPK activation in HepG2 cells treated with OA. Consistent with the *in vivo* decreased in HepG2 cells incubated with 1 mmol/L OA, and this effect was reversed by the KLX treatment; p-AMPK levels were increased from total AMPK protein levels were observed in the control, OA and KLX (10 mol/L) treatment groups (± 0.26results, the levels of the p-AMPK protein were significantly to 1.34 Fig. 4± 0.65 (**A** and Fig. 4Fig. 4**B**). Then, we confirmed the effects of KLX **D D** and and **FE**)). No significant changes in the . $^{-1}$·d^{-1})-almost equivalent to that in the normal cells. No changes were observed efficiently suppress the phosphorylation of AMPK (Thr-172); however, in the total AMPK (t-AMPK) protein expression (when the activation of AMPK was inhibited by compound C and became AMPK, we used compound C (a specific inhibitor of AMPK) to inhibit SREBP-2/PCSK9/LDLR signalling pathway depend on the activation of KLX markedly increased the protein expression of p-AMPK (Thr-172) compared with that in the normal cells The

effect of KLX was blocked AMPK activation in HepG2 cells. The data indicate that compound C can To elucidate whether the effects of KLX on the regulation of the Then, we investigate whether the activation of AMPK is necessary for Fig. 6**A**–**C**).

KLX to influence the SREBP-2/PCSK9/LDLR signalling pathway. The *3.5. KLX regulates SREBP-2/PCSK9/LDLR signalling pathway in the liver* data indicate that the expression levels of SREBP-2 mRNA and P-SREBP- *of hyperlipidaemic rats and OA-treated hepatocytes* 2, N-SREBP-2 and PCSK9 proteins were significantly increased and the levels of the LDLR protein were decreased when AMPK was blocked by

AMPK inhibits the protein expression of sterol regulatory element compound C. Similarly, KLX administration alone was able to reduce the binding protein 2 (SREBP-2) *via* direct phosphorylation [26] and expression levels of SREBP-2 mRNA and P-SREBP-2, N-SREBP-2 and downregulates proprotein convertase subtilisin/kexin type 9 (PCSK9) PCSK9 proteins and enhance the LDLR protein expression compared expression, in turn increasing the level of the low density lipoprotein with that in the normal cells. However, the effect of KLX on the SREBP-

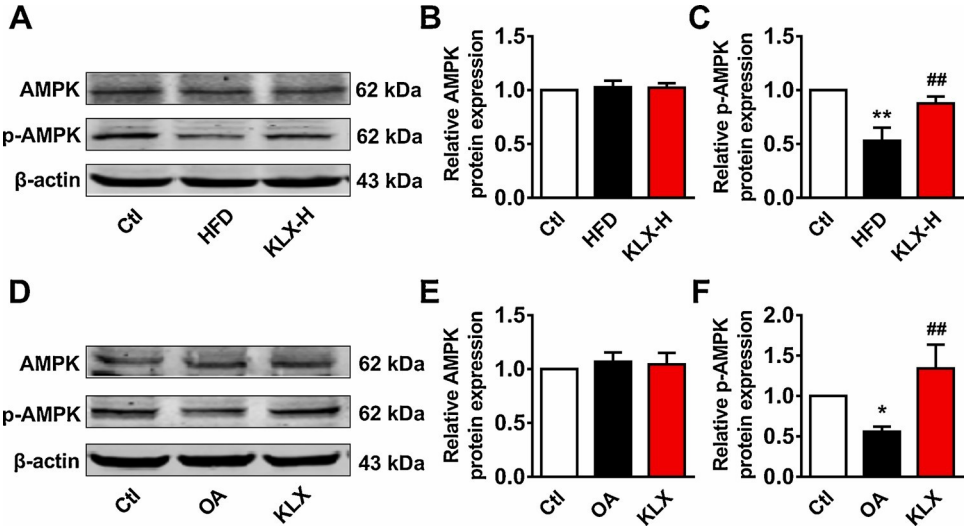

Fig. 4. Kanglexin Promotes AMPK Activation. (A-C) The protein expression levels of phosphorylated-AMPK (p-AMPK) and total- AMPK (AMPK) in the livers of normal diet-fed rats (Ctl), hyperlipidemic rats (HFD) and HFD rats treated with Kanglexin (KLX). All values are presented as the mean ± SEM; $n = 6$, $^{**}P < 0.01$ *vs.* Ctl, $^{\#\#}P < 0.01$ *vs.* HFD. **(D-F)** The protein expression levels of phosphorylated- AMPK (p-AMPK) and total-AMPK (AMPK) in normal hepatocytes (Ctl), dyslipidemic hepatocytes induced by oleic acid (OA), and KLX- treated hepatocytes. All values are presented as the mean ± SEM; $n = 4$, $^{*}P < 0.05$ *vs.* Ctl, $^{\#\#}P < 0.01$ *vs.* OA.

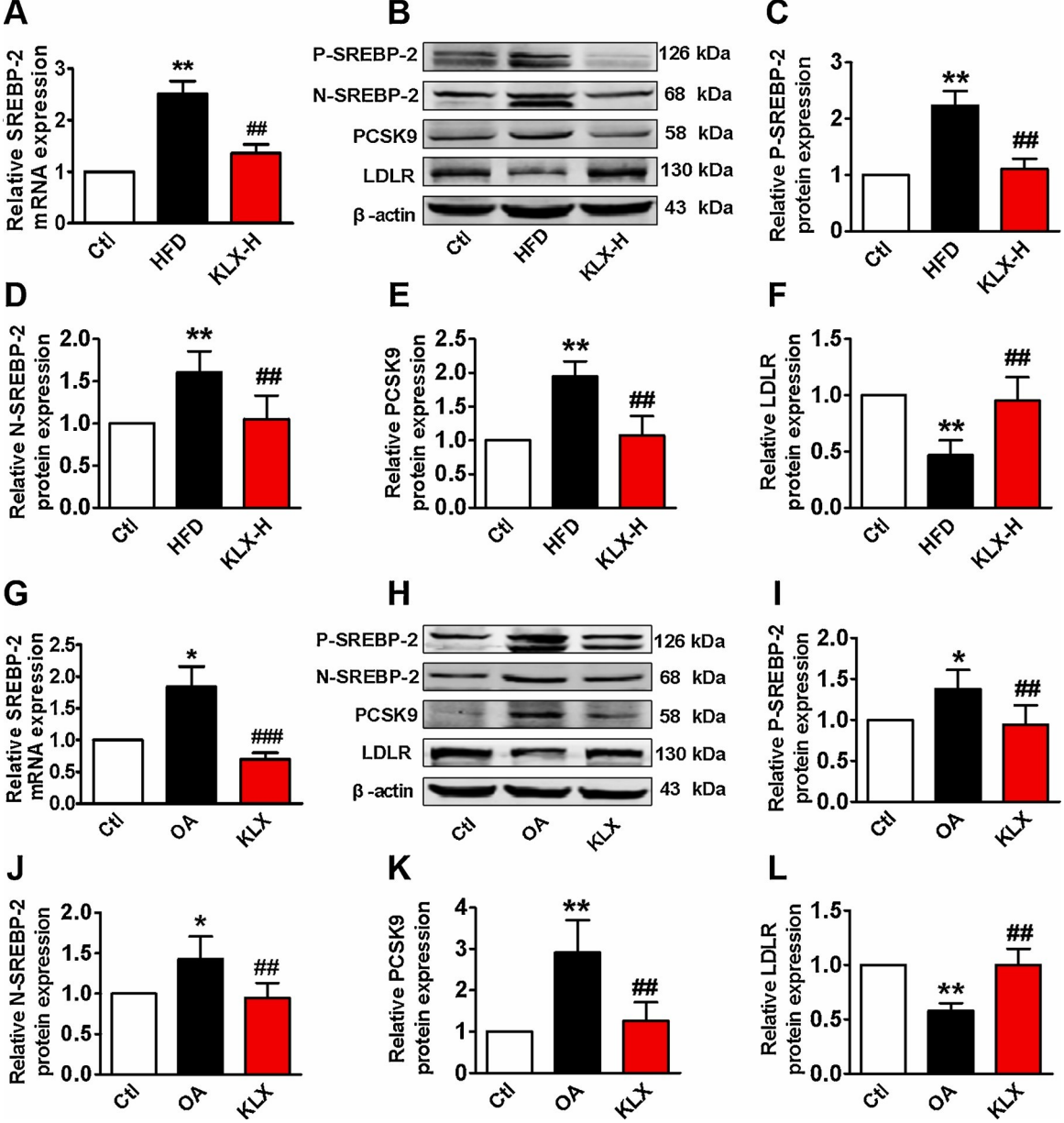

Fig. 5. KLX can regulate the SREBP-2/PCSK9/LDLR signalling pathway in the livers of hyperlipidaemic rats and OA-treated hepatocytes. (A) The relative expression levels of SREBP-2 mRNA in the livers of normal diet-fed rats (Ctl), hyperlipidemic rats (HFD) and Kanglexin treated rats (KLX). **(B)** The representative western blot bands of the P-SREBP-2, N-SREBP-2, PCSK9 and LDLR proteins in the livers of rats in the Ctl, HFD and KLX groups. (C–F) The relative protein expression levels of P-SREBP-2, N-SREBP-2, PCSK9 and LDLR in the livers of rats in the Ctl, HFD and KLX groups. All values are presented as the mean ± SEM; $n = 3$ or 6, $^{**}P < 0.01$ *vs.* Ctl, $^{\#\#}P < 0.01$ *vs.* HFD. **(G)** The relative expression levels of SREBP-2 mRNA in hepatocytes of the Ctl, OA and KLX groups. (H) The representative western blot bands of the P-SREBP-2, N-SREBP-2, PCSK9 and LDLR proteins of normal hepatocytes (Ctl), dyslipidemic hepatocytes induced by oleic acid (OA), and KLX- treated hepatocytes (KLX). (I–L) The relative protein expression levels of P-SREBP-2, N-SREBP-2, PCSK9 and LDLR in hepatocytes of the Ctl, OA and KLX groups. All values are presented as the mean ± SEM; $n = 4$ - 6, $^{*}P < 0.05$, $^{**}P < 0.01$ *vs.* Ctl, $^{\#\#}P < 0.01$, $^{\#\#\#}P < 0.001$ *vs.* OA. P-SREBP-2: precursor of sterol regulatory element binding protein 2; N-SREBP-2: active nuclear sterol regulatory element binding protein 2; PCSK9: proprotein convertase subtilisin/kexin type 9; LDLR: low-density lipoprotein receptor.

2/PCSK9/LDLR signalling pathway, the downstream pathway of AMPK, was blocked upon co-incubation of compound C and KLX (Fig. 6**D–I**). These data indicate that KLX functions through the AMPK/SREBP-2/ PCSK9/LDLR signalling pathway.

4. Discussion

Hyperlipidaemia is a metabolic disease that has become a major global public health problem [28]. In the present study, we designed and synthesized a new anthraquinone compound 1,8-dihydroxy-3-succinic acid monoethyl ester-6-methylanthraquinone and named it Kanglexin (KLX); KLX exhibits a substantial lipid-lowering effect. KLX dramatically reduces the serum TC, TG, and LDL-c levels and hepatic TC and TG levels, ameliorates liver damage and attenuates lipid accumulation in rats with hyperlipidaemia. Additionally, KLX reduces the lipid accumulation and TC and TG contents in the hyperlipidaemic HepG2 cells stimulated with OA. Furthermore, KLX activates AMPK by promoting AMPK phosphorylation at Thr-172 and thus regulates the downstream targets SREBP-2, PCSK9 and LDLR to improve hepatic lipid metabolism. Activation of the AMPK/SREBP-2/PCSK9/LDLR signalling pathway may

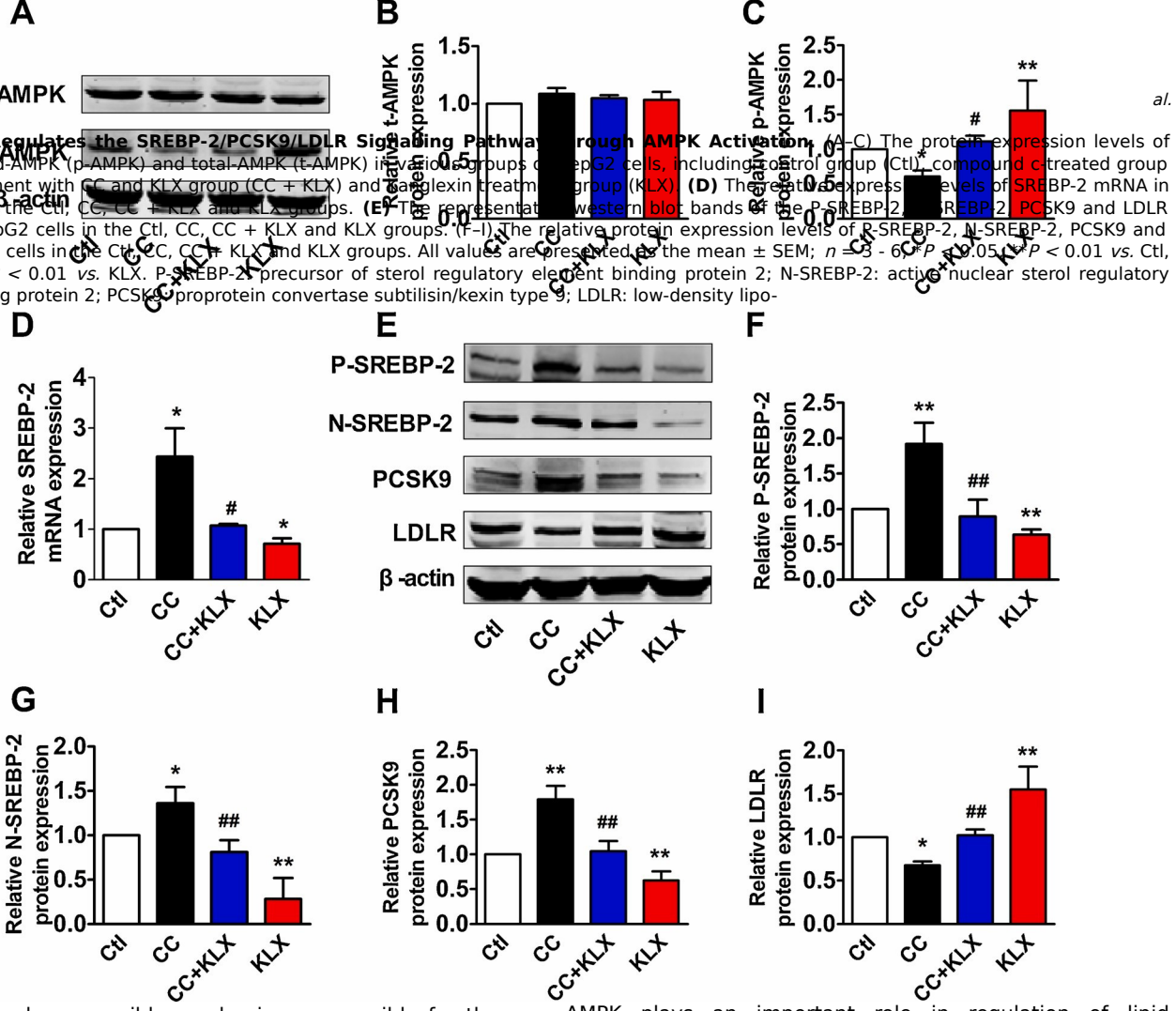

Fig. 6. KLX Regulates the SREBP-2/PCSK9/LDLR Signalling Pathway through AMPK Activation. (A–C) The protein expression levels of phosphorylated-AMPK (p-AMPK) and total-AMPK (t-AMPK) in various groups of HepG2 cells, including control group (Ctl), compound c-treated group (CC), co-treatment with CC and KLX group (CC + KLX) and ganglexin treatment group (KLX). **(D)** The relative expression levels of SREBP-2 mRNA in HepG2 cells of the Ctl, CC, CC + KLX and KLX groups. **(E)** The representative western blot bands of the P-SREBP-2, N-SREBP-2, PCSK9 and LDLR proteins of HepG2 cells in the Ctl, CC, CC + KLX and KLX groups. (F–I) The relative protein expression levels of P-SREBP-2, N-SREBP-2, PCSK9 and LDLR in HepG2 cells in the Ctl, CC, CC + KLX and KLX groups. All values are presented as the mean ± SEM; $n = 3$ - 6; $^{*}P < 0.05$, $^{**}P < 0.01$ *vs.* Ctl, $^{\#}P < 0.05$, $^{\#\#}P < 0.01$ *vs.* KLX. P-SREBP-2: precursor of sterol regulatory element binding protein 2; N-SREBP-2: active nuclear sterol regulatory element binding protein 2; PCSK9: proprotein convertase subtilisin/kexin type 9; LDLR: low-density lipoprotein receptor.

be a possible mechanism responsible for the hypolipidaemic effect of KLX.

AMP-activated protein kinase (AMPK) is a heterotrimeric complex composed of one catalytic α-subunit and two regulatory β- and γ-subunits. The N-terminal portion of the α catalytic subunit of AMPK has a serine/threonine protein kinase domain and the C-terminal region contains the β- and γ-binding domain required for the formation of the heterotrimer complex [29,30]. Activation of AMPK usually occurs on the α-subunit; multiple sites in the α-subunit (Thr 172, Thr 258, Ser 485, *etc.*) can be phosphorylated, and Thr 172 phosphorylation is considered as a biomarker of AMPK activation [31]. According to Bonglee Kim et al., a *Hovenia dulcis* extract inhibits hepatic lipid accumulation by activating AMPK to prevent nonalcoholic fatty liver disease and hyperlipidaemia [35]. Liu SH et al. demonstrated that in high fat diet rats, AMPK activation was inhibited and p-AMPK levels were significantly reduced, while resistant maltodextrin can improve lipid homeostasis by activating AMPK [36]. Xie J et al. found that *Moringa oleifera* leaf petroleum ether extract inhibits lipogenesis by activating the AMPK signalling pathway [37]. In the present study, we found that there was no significant difference in the expression of total AMPK; however, the p-AMPK protein levels were dramatically reduced in rats with hyperlipidaemia and hyperlipidaemic HepG2 cells, and KLX restored the activation of AMPK. Moreover, in HepG2 cells, KLX can promote the expression of p-AMPK protein; however, when AMPK was blocked by compound C, this effect of KLX disappeared, indicating that KLX can activate AMPK.

AMPK plays an important role in regulation of lipid metabolism through phosphorylation of various substrates and influence on multiple downstream targets that are involved in stimulation of fatty acid oxidation, uptake and lipolysis while reducing the cholesterol and fatty acid synthesis [23,32–34]. Hormone-sensitive lipase (HSL) is the key rate-limiting enzyme regulating lipolysis. AMPK activator 5-aminoimidazole-4-carboxamide ribonucleoside (AICAR) can inhibit β-adrenergic-induced lipolysis and this inhibition involves inhibitory phosphorylation of HSL at Ser565 [38,39]. Due to the effects on the cholesterol and fatty acids synthesis, AMPK inhibits the synthesis of cholesterol through phosphorylation of 3-hydroxy-3-methylglutaryl-CoA reductase (HMGCR) at Ser872 thus reducing mevalonic acid modification by acetyl-CoA [40,41]. Furthermore, phosphorylation of acetyl-CoA carboxylase 1 (ACC1) and ACC2 are required for the inhibitory effects of AMPK on fatty acid synthesis [42–44]. In addition to the regulation of cholesterol and fatty acid synthesis through phosphorylation of HMGCR and ACC, AMPK also inhibits this signalling pathway through distinct sterol-response element-binding proteins (SREBPs) [34]. According to a previous study, AMPK can directly phosphorylate SREBP and thus influence proteolytic processing and transcriptional activity of SREBP, which will subsequently suppress the SREBP-mediated gene expression [23]. AMPK can phosphorylate Ser372 and Ser374 on SREBP1C and SREBP2, respectively [34]. SREBP is synthesized in the endoplasmic reticulum (ER) membrane as a precursor protein (P-SREBP). Then, the SREBP precursor migrates from the ER to the Golgi apparatus and is subjected to two-step proteolytic processing by two enzymes that generate a soluble N-terminal basic helix-loop-helix (bHLH)-Zip domain. After maturation, the active nuclear SREBP protein

enters the nucleus (N-SREBP), where it binds to the sterol regulatory element (SRE) and promotes the transcription of the lipogenic genes [45–47]. In fatty acid metabolism, ATP-citrate lyase (ACLY), ACC and fatty acid synthase (FASN) are regulated by SREBP1A and SREBP1C [48]. SREBP-2 regulates cholesterol homeostasis by inducing the expression of the genes required for cholesterol synthesis and uptake [49]. HMGCR and low-density lipoprotein (LDL) receptor are regulated by the activity of SREBP2. Studies have shown that SREBP-2 expression was significantly increased in high fat diet obesity rats [50]; overexpression of SREBP-2 can significantly increase the deposition of lipids and the expression of the genes involved in lipid synthesis and metabolism [51].

Jeong HJ et al. identified an SRE-binding site for SREBP-2 localized in the promoter region of proprotein convertase subtilisin/kexin type 9 (PCSK9) and showed that SREBP-2 increases the promoter activity of PCSK9 [52]. PCSK9 is a secreted serine protease that regulates cholesterol homoeostasis by inducing the internalization and degradation of hepatic low density lipoprotein receptor (LDLR) [53,54]. Graham MJ demonstrated that administration of a PCSK9 antisense oligonucleotide to high fat diet mice for 6 weeks reduced total cholesterol and LDL by 53 % and 38 %, respectively. Moreover, inhibition of PCSK9 expression resulted in a 2-fold increase in hepatic LDLR protein levels [55]. LDLR is a transmembrane glycoprotein that belongs to the low density lipoprotein receptor gene family and is a central molecule that maintains the LDL-c levels and plays a primary role in cholesterol homeostasis [56,57]. Elevated levels of LDL-c are considered a main risk factor for the development of cardiovascular diseases [58]. LDL-c is taken up by the LDLR on the surface of hepatocytes forming LDL-c and LDLR complexes. Then, the complexes are endocytosed into the cells and degraded in lysosomes resulting in the clearance of LDL-c and recycling of LDLR [59, 60].

As shown in the present study, N-SREBP-2 and PCSK9 protein expression levels were increased and LDLR levels was decreased in rats with high fat diet-induced hyperlipidaemia and in OA-induced HepG2 cells with lipid depositions and these conditions were reversed by KLX. Moreover, if AMPK was blocked by compound C in HepG2 cells, the levels of N-SREBP-2 and PCSK9 were significantly increased and the level of LDLR was decreased. KLX administration alone significantly decreased the levels of N-SREBP-2 and PCSK9 proteins and increased the LDLR expression. However, the effect of KLX was abolished when compound C and KLX were co-administered. The mRNA levels of SREBP can be upregulated by nuclear SREBP (N-SREBP) *via* a feed-forward mechanism [61]. Khaleel found that SREBP-2 mRNA expression level was elevated in high far diet rat [50]. We detected the mRNA level of SREBP-2 under various treatment conditions. We found that SREBP-2 mRNA expression level was increased in rats with hyperlipidaemia and OA-treated hepatocytes and these effects were reversed by KLX. The effect of KLX was blocked by CC after the treatment with CC and KLX.
This result can explain the changes in the P-SREBP-2 protein under the similar conditions. Therefore, our study suggests that KLX can activate AMPK and its downstream SREBP-2/PCSK9/LDLR signalling pathway. These data may explain the beneficial effects of KLX on lowering lipid accumulation and protection against hyperlipidaemia.

In summary, in the current study, we identified a newly synthesized compound KLX that can attenuate lipid accumulation through activation of the AMPK/SREBP-2/PCSK9/LDLR signalling pathway. These findings may provide molecular evidence for use of Kanglexin in the treatment of hyperlipidaemia or fatty liver.

However, there are certain limitations of this study. We did not determine the ED_{50} of KLX in the present work. Three dose of KLX used in the rats with hyperlipidaemia were 20, 40, and 80 mg $kg^{-1}.d^{-1}$. The dose of the lipid-regulating drug (AT) was 10 mg $kg^{-1}.d^{-1}$, which is routinely selected in similar studies. However, we did not compare the potency of KLX and AT. Therefore, the use of these two drugs at different dose cannot indicate that KLX is a less potent compound than other drugs, such as AT [62–64]. The potency of KLX needs to be determined. Although AMPK exerts its function on the lipid metabolism *via* multiple downstream targets and pathways, we studied only the effect on the SREBP-2/PCSK9/LDLR pathway of regulation of lipid synthesis and uptake. Other downstream proteins, especially SREBP-1, may also be involved in the function of KLX and its activation of AMPK, which requires further investigation.

5. Conclusions

Kanglexin (KLX) is a new anthraquinone compound that functions by lowering blood lipids and alleviating hepatic lipid accumulation; these effects may be relates to activation of the AMPK/SREBP-2/PCSK9/LDLR signalling pathway.

Authorship contributions

Participated in research design: Yang; Conducted experiments: Li, N Wang and Zhang; Contributed new reagents or analytic tools: Yang, JH Wang and ZZ Wang; Performed data analysis: Li, Hu and Dong; Wrote or contributed to the writing of the manuscript: Li, Hu and N Wang; Participated in the experiments: Hu, Pan, Dong, Ding, Song, XZ Wang.

Funding

This work was supported by the Key Project of the National Natural Science Foundation of China [Grants 81730012], the China-Canada Cooperation Project of the National Natural Science Foundation of China [Grants 81861128022], and the University Nursing Program for Young Scholars with Creative Talents in Heilongjiang Province (UNPYSCT-2016051).

Declaration of Competing Interest

The authors declare that there are no conflicts of interests.

Appendix A. Supplementary data

Supplementary material related to this article can be found, in the online version, at doi:https://doi.org/10.1016/j.biopha.2020.110802.

References

[1] J. Najib, Fenofibrate in the treatment of dyslipidemia: a review of the data as they relate to the new suprabioavailable tablet formulation, Clin. Ther. 24 (December (12)) (2002) 2022–2050, https://doi.org/10.1016/s0149-2918(02)80095-9.
[2] L. Dupuis, P. Corcia, A. Fergani, et al., Dyslipidemia is a protective factor in amyotrophic lateral sclerosis, Neurology 70 (13) (2008) 1004–1009, https://doi. org/10.1212/01.wnl.0000285080.70324.27.

[3] J.L. Goldstein, M.S. Brown, Hyperlipidemia in coronary heart disease: a biochemical genetic approach, J. Lab. Clin. Med. 85 (1) (1975) 15–25.
[4] J.S. Meyer, R.L. Rogers, K.F. Mortel, B.W. Judd, Hyperlipidemia is a risk factor for decreased cerebral perfusion and stroke, Arch. Neurol. 44 (4) (1987) 418–422, https://doi.org/10.1001/archneur.1987.00520160052014.
[5] K.J. van Hateren, N. Kleefstra, Five-year incidence of type 2 diabetes mellitus in patients with familial combined hyperlipidaemia, Neth. J. Med. 68 (1) (2010) 332.
[6] A.M. Gotto Jr., Management of dyslipidemia, Am. J. Med. 112 (Suppl 8A) (2002) 10S–18S, https://doi.org/10.1016/s0002-9343(02)01085-9.
[7] M. Ewang-Emukowhate, A.S. Wierzbicki, Lipid-lowering agents, J. Cardiovasc. Pharmacol. Ther. 18 (5) (2013) 401–411, https://doi.org/10.1177/ 1074248413492906.
[8] R.A. Hegele, S. Tsimikas, Lipid-lowering agents, Circ. Res. 124 (3) (2019) 386–404, https://doi.org/10.1161/circresaha.118.313171.
[9] S. Chen, X. Wen, W. Zhang, C. Wang, J. Liu, C. Liu, Hypolipidemic effect of oleanolic acid is mediated by the miR-98-5p/PGC-1β axis in high-fat diet-induced hyperlipidemic mice, FASEB J. 31 (3) (2017) 1085–1096, https://doi.org/ 10.1096/fj.201601022R.
[10] Y. Li, J.G. Jiang, Health functions and structure-activity relationships of natural anthraquinones from plants, Food Funct. 9 (12) (2018) 6063–6080, https://doi. org/10.1039/C8FO01569D.
[11] Q. Huang, G. Lu, H.M. Shen, M.C. Chung, C.N. Ong, Anti-cancer properties of anthraquinones from rhubarb, Med. Res. Rev. 27 (5) (2007) 609–630, https://doi. org/10.1002/med.20094.
[12] A.S. Tikhomirov, A.A. Shtil, A.E. Shchekotikhin, Advances in the discovery of anthraquinone-based anticancer agents, Recent Pat. Anticancer Drug Discov. 13 (2) (2018) 159–183, https://doi.org/10.2174/1574892813666171206123114.
[13] D. Shrimali, M.K. Shanmugam, A.P. Kumar, et al., Targeted abrogation of diverse signal transduction cascades by emodin for the treatment of inflammatory disorders and cancer, Cancer Lett. 341 (2) (2013) 139–149, https://doi.org/ 10.1016/j.canlet.2013.08.023.
[14] K.S. Kwon, J.H. Lee, K.S. So, et al., Aurantio-obtusin, an anthraquinone from cassiae semen, ameliorates lung inflammatory responses, Phytother. Res. 32 (8) (2018) 1537–1545, https://doi.org/10.1002/ptr.6082.
[15] D.H. Kuo, S.C. Kuo, J.T. Cheng, Structure-activity relationships of anthraquinones in the decrease of intestinal motility, J. Pharm. Pharmacol. 52 (7) (2000) 839–841, https://doi.org/10.1211/0022357001774516.
[16] S.K. Mishra, S. Tiwari, A. Shrivastava, et al., Antidyslipidemic effect and antioxidant activity of anthraquinone derivatives from Rheum emodi rhizomes in dyslipidemic rats, J. Nat. Med. 68 (2) (2014) 363–371, https://doi.org/10.1007/ s11418-013-0810-z.
[17] Y. Li, J.G. Jiang, Health functions and structure-activity relationships of natural anthraquinones from plants, Food Funct. 9 (12) (2018) 6063–6080, https://doi. org/10.1039/C8FO01569D.
[18] E.M. Malik, C.E. Müller, Anthraquinones As pharmacological tools and drugs, Med. Res. Rev. 36 (4) (2016) 705–748, https://doi.org/10.1002/med.21391.
[19] J. Li, W. Yang, J. Chen, A study on extraction of total anthraquinone from Aloe, Acta Agriculturae Universitatis Jiangxiensis. 31 (2009) 545–548, https://doi.org/ 10.1007/s00449-008-0288-3.
[20] B. Jin, W. Li, W. Cai, Studies on extraction and purification process of total rhubarb, Lishizhen Medicine and Materia Medica Res. 16 (2005) 756–758, doi: CNKI:SUN:SZGY.0.2005-08-041.
[21] C. Zhang, Studies on Preparation Process and Quality Standard of Aloe Extract, Henan University, 2008, https://doi.org/10.7666/d.y1269695.
[22] B. Cool, B. Zinker, W. Chiou, et al., Identification and characterization of a small molecule AMPK activator that treats key components of type 2 diabetes and the metabolic syndrome, Cell Metab. 3 (6) (2006) 403–416, https://doi.org/10.1016/j. cmet.2006.05.005.
[23] B. Viollet, F. Andreelli, AMP-activated protein kinase and metabolic control, Handb. Exp. Pharmacol. (203) (2011) 303–330, https://doi.org/10.1007/978-3- 642-17214-4_13.
[24] H.S. Chae, B.H. You, D.Y. Kim, et al., Sauchinone controls hepatic cholesterol homeostasis by the negative regulation of PCSK9 transcriptional network, Sci. Rep. 8 (1) (2018) 6737, https://doi.org/10.1038/s41598-018-24935-6.
[25] J.H. Kang, R. Toita, M. Murata, Liver cell-targeted delivery of therapeutic molecules, Crit. Rev. Biotechnol. 36 (1) (2016) 132–143, https://doi.org/10.3109/ 07388551.2014.930017.
[26] Y. Li, S. Xu, M.M. Mihaylova, et al., AMPK phosphorylates and inhibits SREBP activity to attenuate hepatic steatosis and atherosclerosis in diet-induced insulin- resistant mice, Cell Metab. 13 (4) (2011) 376–388, https://doi.org/10.1016/j. cmet.2011.03.009.
[27] B. Dong, M. Wu, H. Li, et al., Strong induction of PCSK9 gene expression through HNF1alpha and SREBP2: mechanism for the resistance to LDL-cholesterol lowering effect of statins in dyslipidemic hamsters, J. Lipid Res. 51 (6) (2010) 1486–1495, https://doi.org/10.1194/jlr.m003566.
[28] B. Klop, J.W. Elte, M.C. Cabezas, Dyslipidemia in obesity: mechanisms and potential targets, Nutrients 5 (4) (2013) 1218–1240, https://doi.org/10.3390/ nu5041218.
[29] A. Woods, I. Salt, J. Scott, D.G. Hardie, D. Carling, The alpha1 and alpha2 isoforms of the AMP-activated protein kinase have similar activities in rat liver but exhibit differences in substrate specificity in vitro, FEBS Lett. 397 (2-3) (1996) 347–351, https://doi.org/10.1016/S0014-5793(96)01209-4.
[30] B. Xiao, R. Heath, P. Saiu, et al., Structural basis for AMP binding to mammalian AMP-activated protein kinase, Nature 449 (7161) (2007) 496–500, https://doi. org/10.3410/f.1092059.545423.
[31] D.G. Hardie, F.A. Ross, S.A. Hawley, AMPK: a nutrient and energy sensor that maintains energy homeostasis, Nat. Rev. Mol. Cell Biol. 13 (4) (2012) 251–262, https://doi.org/10.1038/nrm3311.
[32] S.H. Liu, C.Y. Chiu, L.H. Huang, M.T. Chiang, Resistant maltodextrin ameliorates altered hepatic lipid homeostasis via activation of AMP-Activated protein kinase in a high-fat diet-fed rat model, Nutrients 11 (2) (2019) 291, https://doi.org/ 10.3390/nu11020291.
[33] B. Kim, M.J. Woo, C.S. Park, et al., Hovenia Dulcis extract reduces lipid accumulation in oleic acid-induced steatosis of Hep G2 cells via activation of AMPK and PPARα/CPT-1 pathway and in acute hyperlipidemia mouse model, Phytother. Res. 31 (1) (2017) 132–139, https://doi.org/10.1002/ptr.5741.
[34] J. Xie, Y. Wang, W.W. Jiang, et al., Moringa oleifera leaf petroleum ether extract inhibits lipogenesis by activating the AMPK signaling pathway, Front. Pharmacol. 8 (2018) 1447, https://doi.org/10.3389/fphar.2018.01447.
[35] M.D. Fullerton, AMP-activated protein kinase and its multifaceted regulation of hepatic metabolism, Curr. Opin. Lipidol. 27 (2) (2016) 172–180, https://doi.org/ 10.1097/mol.0000000000000273.
[36] S.M. Jeon, Regulation and function of AMPK in physiology and diseases, Exp. Mol. Med. 48 (7) (2016) e245, https://doi.org/10.1038/emm.2016.81.
[37] G.R. Steinberg, D. Carling, AMP-activated protein kinase: the current landscape for drug development, Nat. Rev. Drug Discov. 18 (7) (2019) 527–551, https://doi.org/ 10.1038/s41573-019-0019-2.
[38] J.M. Corton, J.G. Gillespie, S.A. Hawley, D.G. Hardie, 5-Aminoimidazole-4- carboxamide ribonucleoside. A specific method for activating AMP-activated protein kinase in intact cells? Eur. J. Biochem. 229 (1995) 558–565, https://doi. org/10.1111/j.1432-1033.1995.tb20498.x.
[39] J.E. Sullivan, et al., Inhibition of lipolysis and lipogenesis in isolated rat adipocytes with AICAR, a cell-permeable activator of AMP-activated protein kinase, FEBS Lett. 353 (1994) 33–36, https://doi.org/10.1016/0014-5793(94)01006-4.
[40] S.C. Lin, D.G. Hardie, AMPK: sensing glucose as well as cellular energy status, Cell Metab. 27 (2018) 299–313, https://doi.org/10.1016/j.cmet.2017.10.009.
[41] T.S. Ingebritsen, M.J. Geelen, R.A. Parker, K.J. Evenson, D.M. Gibson, Modulation of hydroxymethylglutaryl-CoA reductase activity, reductase kinase activity, and cholesterol synthesis in rat hepatocytes in response to insulin and glucagon, J. Biol. Chem. 254 (1979) 9986–9989.
[42] R.M. Esquejo, et al., Activation of liver AMPK with PF-06409577 corrects NAFLD and lowers cholesterol in rodent and primate preclinical models, EBioMedicine 31 (2018) 122–132, https://doi.org/10.1016/j.ebiom.2018.04.009.
[43] M.D. Fullerton, et al., Single phosphorylation sites in Acc1 and Acc2 regulate lipid homeostasis and the insulin-sensitizing effects of metformin, Nat. Med. 19 (2013) 1649–1654, https://doi.org/10.1038/nm.3372.
[44] H.M. O'Neill, et al., AMPK phosphorylation of ACC2 is required for skeletal muscle fatty acid oxidation and insulin sensitivity in mice, Diabetologia 57 (2014) 1693–1702, https://doi.org/10.1007/s00125-014-3273-1.
[45] M.S. Brown, J.L. Goldstein, A proteolytic pathway that controls the cholesterol content of membranes, cells, and blood, Proc. Natl. Acad. Sci. U. S. A. 96 (20) (1999) 11041–11048, https://doi.org/10.1073/pnas.96.20.11041.
[46] J. Kotzka, B. Knebel, H. Avci, et al., Phosphorylation of sterol regulatory element- binding protein (SREBP)-1a links growth hormone action to lipid metabolism in hepatocytes, Atherosclerosis 213 (1) (2010) 156–165, https://doi.org/10.1016/j. atherosclerosis.2010.08.046.
[47] X. Xu, J.S. So, J.G. Park, A.H. Lee, Transcriptional control of hepatic lipid metabolism by SREBP and ChREBP, Semin. Liver Dis. 33 (4) (2013) 301–311, https://doi.org/10.1055/s-0033-1358523.
[48] J. Ye, R.A. DeBose-Boyd, Regulation of cholesterol and fatty acid synthesis, Cold Spring Harb. Perspect. Biol. 3 (2011), a004754, https://doi.org/10.1101/ cshperspect.a004754.
[49] R. Sato, Sterol metabolism and SREBP activation, Arch. Biochem. Biophys. 501 (2) (2010) 177–181, https://doi.org/10.1016/j.abb.2010.06.004.
[50] E.F. Khaleel, G.A. Abdel-Aleem, D.G. Mostafa, Resveratrol improves high-fat diet induced fatty liver and insulin resistance by concomitantly inhibiting proteolytic cleavage of sterol regulatory element-binding proteins, free fatty acid oxidation, and intestinal triglyceride absorption,

Can. J. Physiol. Pharmacol. 96 (2) (2018) 145–157, https://doi.org/10.1139/cjpp-2017-0001.
[51] P. Malhotra, C. Aloman, A. Ankireddy, et al., Overactivation of intestinal sterol response element-binding protein 2 promotes diet-induced nonalcoholic steatohepatitis, Am. J. Physiol. Gastrointest. Liver Physiol. 313 (5) (2017) G376–G385, https://doi.org/10.1152/ajpgi.00174.2017.
[52] H.J. Jeong, H.S. Lee, K.S. Kim, Y.K. Kim, D. Yoon, S.W. Park, Sterol-dependent regulation of proprotein convertase subtilisin/kexin type 9 expression by sterol- regulatory element binding protein-2, J. Lipid Res. 49 (2) (2008) 399–409, https:// doi.org/10.1194/jlr.m700443-jlr200.
[53] J. Li, C. Tumanut, J.A. Gavigan, et al., Secreted PCSK9 promotes LDL receptor degradation independently of proteolytic activity, Biochem. J. 406 (2) (2007) 203–207, https://doi.org/10.1042/BJ20070664.
[54] C.E. Kosmas, E. DeJesus, R. Morcelo, F. Garcia, P.D. Montan, E. Guzman, Lipid- lowering interventions targeting proprotein convertase subtilisin/kexin type 9 (PCSK9): an emerging chapter in lipid-lowering therapy, Drugs Context 6 (2017), 212511, https://doi.org/10.7573/dic.212511.
[55] M.J. Graham, K.M. Lemonidis, C.P. Whipple, et al., Antisense inhibition of proprotein convertase subtilisin/kexin type 9 reduces serum LDL in hyperlipidemic mice, J. Lipid Res. 48 (4) (2007) 763–767, https://doi.org/10.1194/jlr.c600025- jlr200.
[56] L.J. Sharpe, A.J. Brown, Rapamycin down-regulates LDL-receptor expression independently of SREBP-2, Biochem. Biophys. Res. Commun. 373 (4) (2008) 670–674, https://doi.org/10.1016/j.bbrc.2008.06.108.
[57] L. Jia, N. Song, G. Yang, et al., Effects of Tanshinone IIA on the modulation of miR-33a and the SREBP-2/Pcsk9 signaling pathway in hyperlipidemic rats, Mol. Med. Rep. 13 (6) (2016) 4627–4635, https://doi.org/10.3892/mmr.2016.5133.
[58] Chen W. Yu KC, A.D. Cooper, LDL receptor-related protein mediates cell-surface clustering and hepatic sequestration of chylomicron remnants in LDLR-deficient mice, J. Clin. Invest. 107 (11) (2001) 1387–1394, https://doi.org/10.1172/ JCI11750.
[59] S. Hirayama, T. Miida, Small dense LDL: an emerging risk factor for cardiovascular disease, Clin. Chim. Acta 414 (2012) 215–224, https://doi.org/10.1016/j. cca.2012.09.010.
[60] P. Abidi, Y. Zhou, J.D. Jiang, J. Liu, Extracellular signal-regulated kinase-dependent stabilization of hepatic low-density lipoprotein receptor mRNA by herbal medicine berberine, Arterioscler. Thromb. Vasc. Biol. 25 (10) (2005) 2170–2176, https://doi.org/10.1161/01.ATV.0000181761.16341.2b.
[61] G. Garab, Z. Cseh, L. Kovacs, et al., Light-induced trimer to monomer transition in ´ the main light-harvesting antenna complex of plants: thermo-optic mechanism, Biochemistry. 41 (51) (2002) 15121–15129, https://doi.org/10.1021/bi026157g.
[62] Y. Bian, X. Li, X. Li, et al., Daming capsule, a hypolipidaemic drug, lowers blood lipids by activating the AMPK signalling pathway, Biomed. Pharmacother. 117 (2019), 109176, https://doi.org/10.1016/j.biopha.2019.109176.
[63] S. Ding, J. Kang, L. Tong, Y. Lin, L. Liao, B. Gao, Erchen decoction ameliorates lipid metabolism by the regulation of the protein CAV-1 and the receptors VLDLR, LDLR, ABCA1, and SRB1 in a high-fat diet rat model, Evid. Complement. Alternat. Med. 2018 (2018), 5309490, https://doi.org/10.1155/2018/5309490.
[64] J. Gao, C. Liu, H. Zhang, Z. Sun, R. Wang, Myricitrin exhibits anti-atherosclerotic and anti-hyperlipidemic effects in diet-induced hypercholesterolemic rats, AMB Express 9 (1) (2019) 204, https://doi.org/10.1186/s13568-019-0924-0.